

Supplementary Information for

Free energy landscapes from SARS-CoV-2 spike glycoprotein simulations suggest that RBD opening can be modulated via interactions in an allosteric pocket

Lucy Fallon^{1,2#}, Kellon A.A. Belfon^{1,2#}, Lauren Raguette^{1,2}, Yuzhang Wang^{1,2}, Darya Stepanenko^{1,4}, Abbigayle Cuomo², Jose Guerra⁵, Stephanie Budhan², Sarah Varghese⁶, Christopher Corbo³, Robert C. Rizzo^{1,4}, and Carlos Simmerling^{1,2*}

¹Laufer Center for Physical and Quantitative Biology, Stony Brook University, Stony Brook, New York 11794, United States

²Department of Chemistry, Stony Brook University, Stony Brook, New York 11794, United States

³Graduate Program in Molecular and Cellular Pharmacology, Stony Brook University, Stony Brook, New York 11794, United States

⁴Department of Applied Mathematics and Statistics, Stony Brook University, Stony Brook, New York 11794, United States

⁵Department of Biochemistry and Cell Biology, Stony Brook University, Stony Brook, New York 11794, United States

⁶Undergraduate Program in Biology, Stony Brook University, Stony Brook, New York 11794, United States

These authors contributed equally to this work.

Organization

1. Figures
 2. Tables
 3. References
-

1. Figures

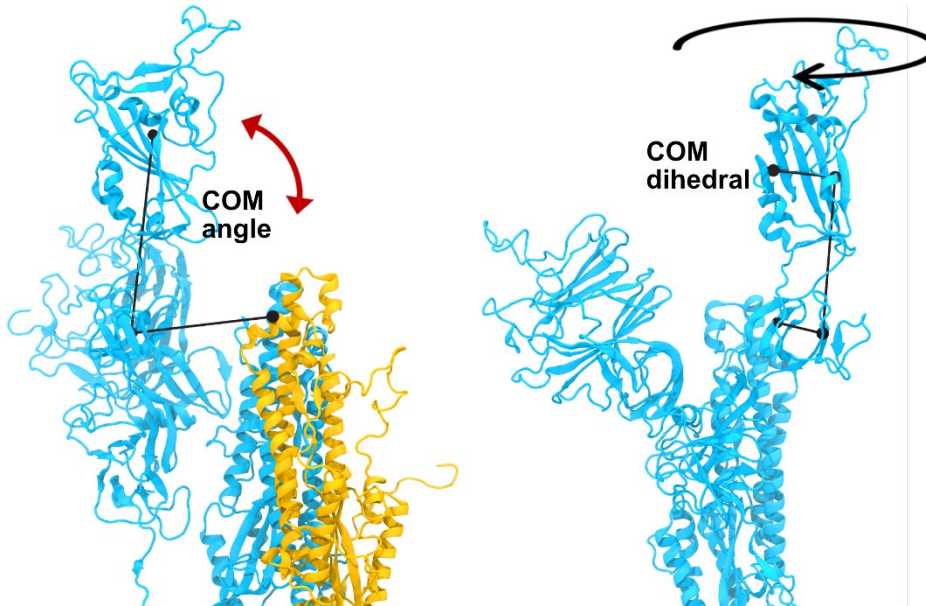


Figure S1—Center of mass (COM) based collective variables (CVs) used to quantify RBD motion relative to the remainder of the spike. (Left) the COM angle measures movement of the RBD up and away from the core central helices, and (right) the COM dihedral measures rotation of the RBD relative to the CTD1 domain. Portions of 2 protomers are shown, with coloring matching **Figure 4**. Amino acid ranges used to define the COM groups (black circles) are shown in **Table S4**. Additional details are provided in Methods.

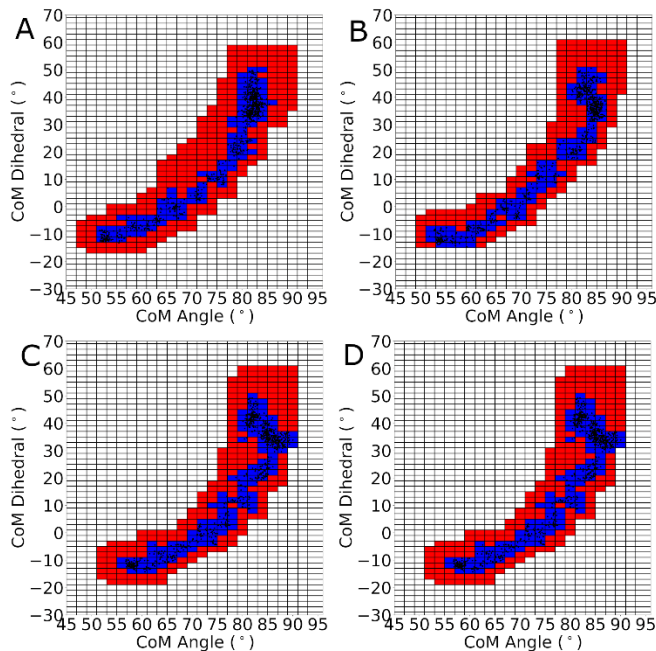


Figure S2: 2D grid of CoM angle and CoM dihedral collective variables. The colored grids were used as windows for US simulations to calculate the free energy for RBD opening in A) WT, B) K528A, C) A522L, and D) A522V S-protein. The initial grids used as US windows before grid expansion are shown in blue, additional grids used as new windows for expansion are shown in red. The SMD trajectory snapshots are mapped onto the 2D grid as black dots.

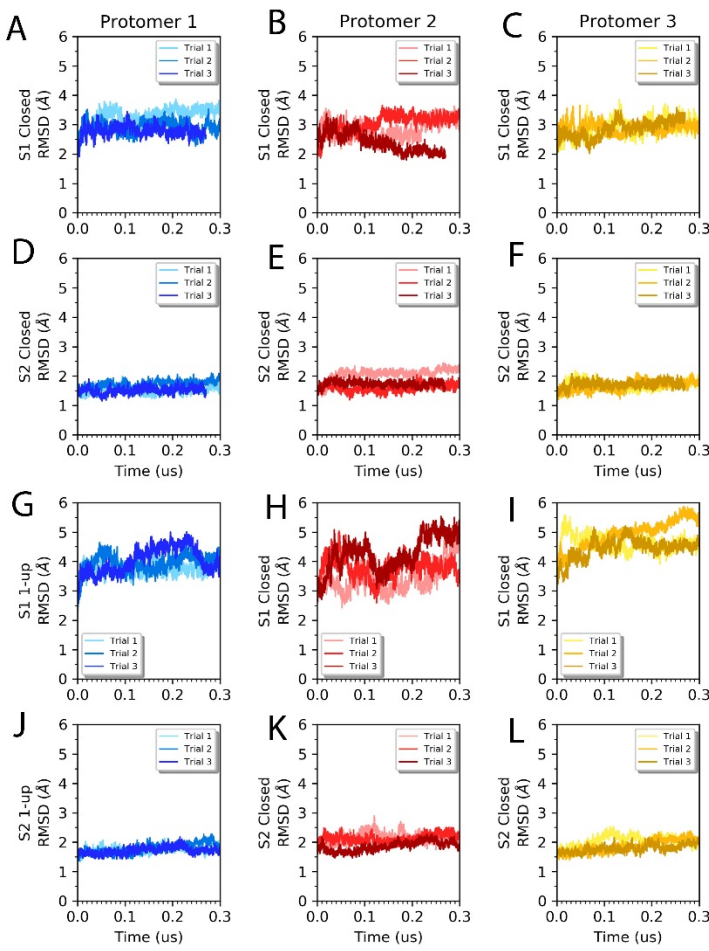


Figure S3. RMSD of backbone atoms of each protomer (blue, red, yellow) over three MD runs of the spike over 270, 300 and 300 ns. (A,B,C) S1, closed spike system; (D,E,F) S2, closed; (G,H,I) S1, 1-up; (J,K,L) S2, 1-up. Each shade in a plot represents one of three independent trials. Columns represent protomers 1, 2 and 3 with colors matching **Figure 4**. RMSD is relative to the respective reference structure.

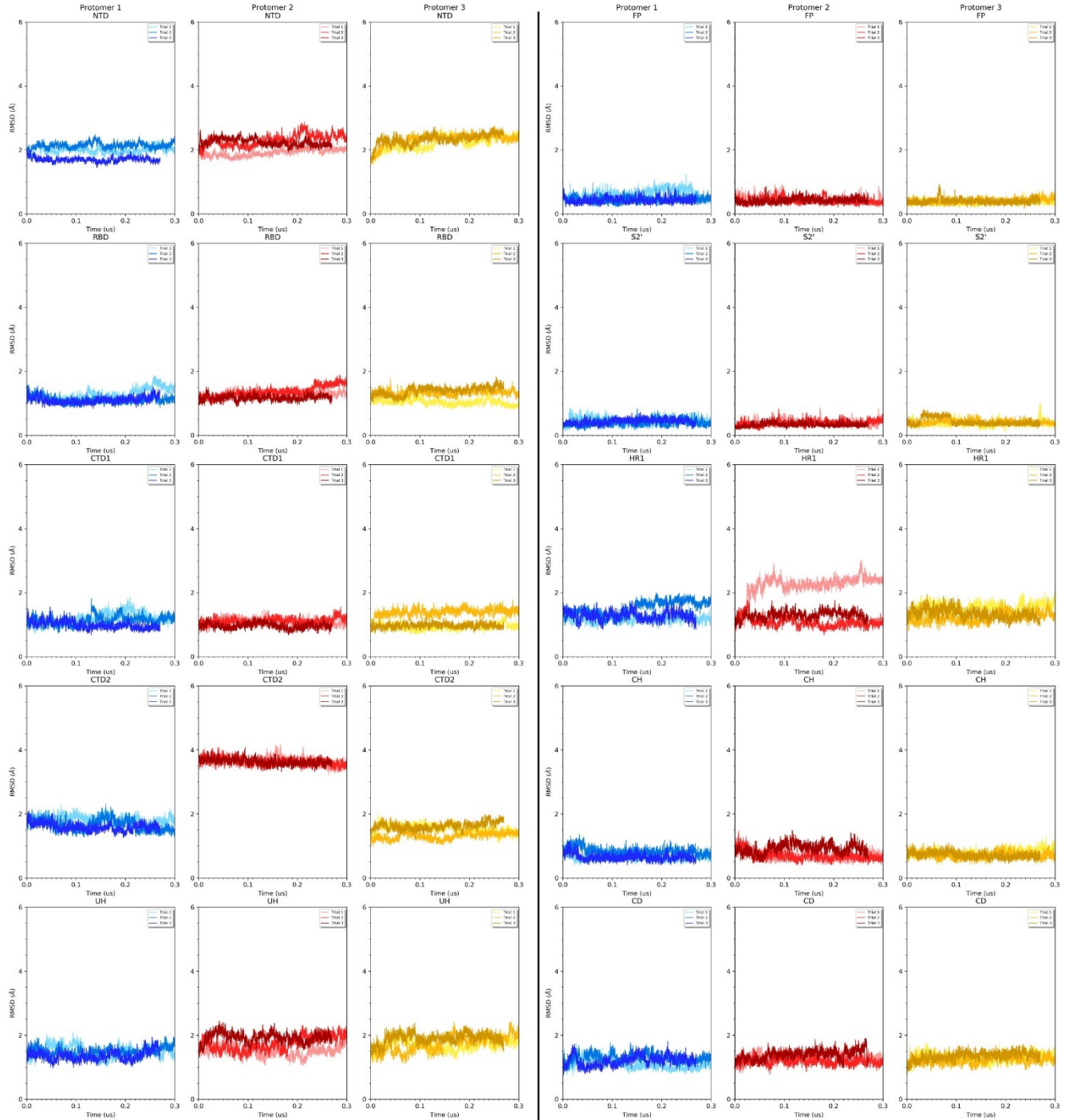


Figure S4. Domain RMSDs during MD simulations of the closed spike. Residue ranges for each domain are provided in Table S3. Rows correspond to specific domains. Columns show data for each protomer, with 3 independent runs in different shades. RMSD is relative to the respective reference structure.

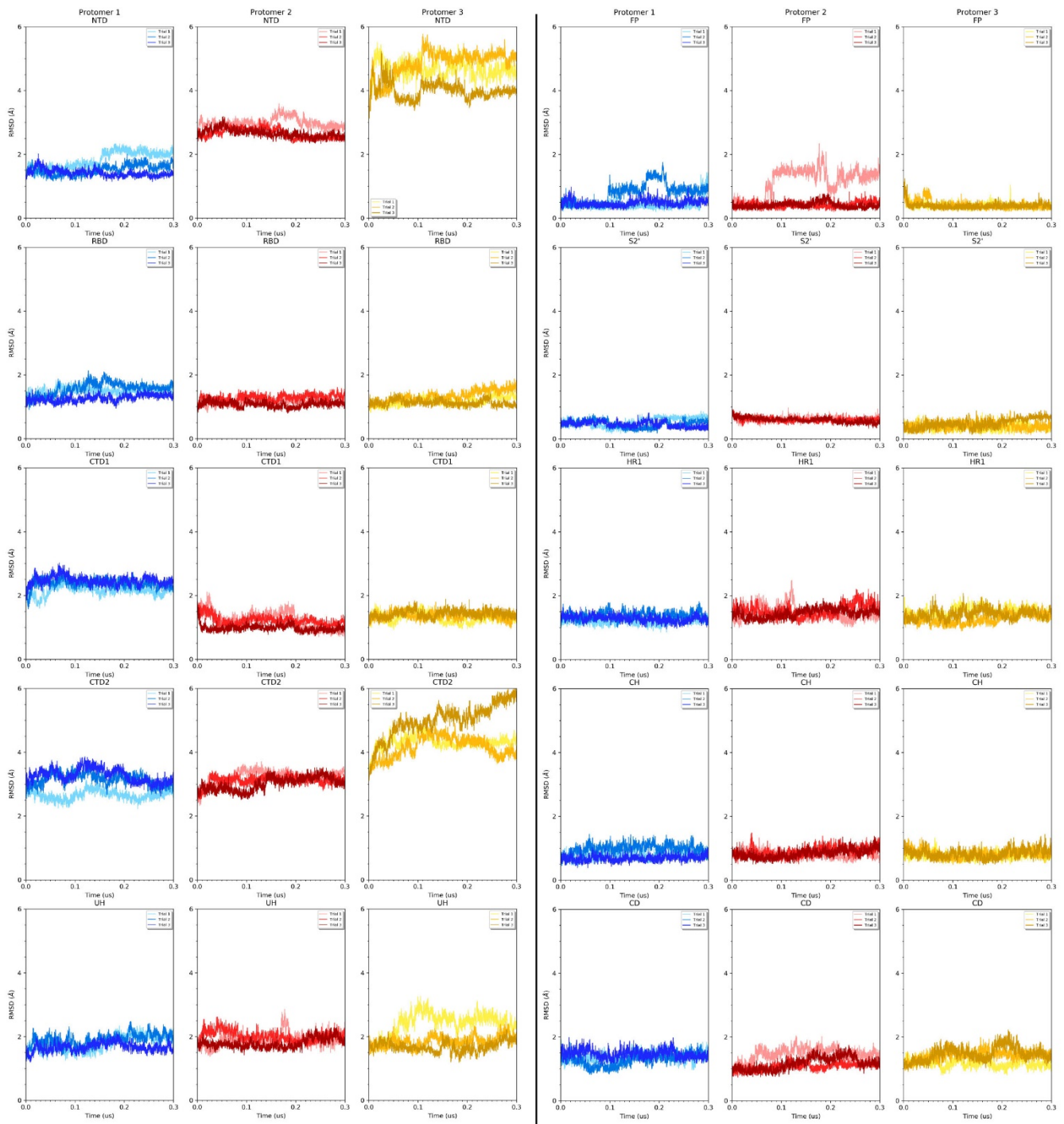


Figure S5. Domain RMSDs during MD simulations of the 1-up spike. Residue ranges for each domain are provided in Table S3. Columns show data for each protomer, with 3 independent runs in different shades. Protomer 1 has the RBD in the open position. RMSD is relative to the respective reference structure.

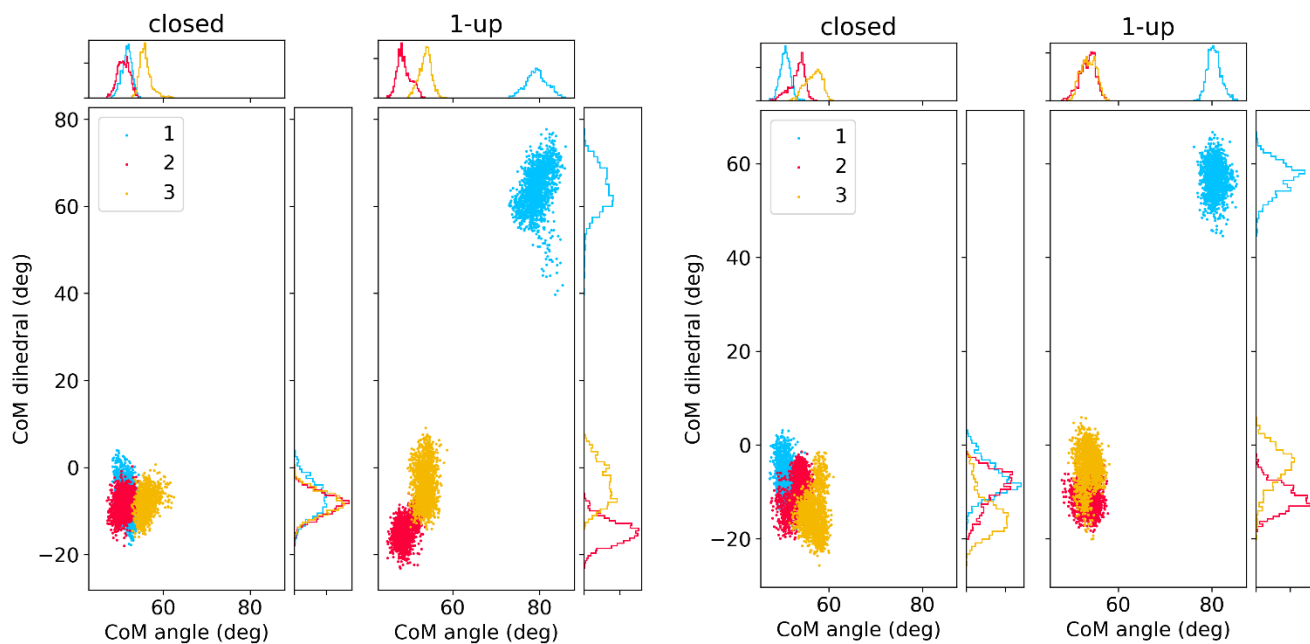


Figure S6. Collective variables for 2 additional independent runs of closed and 1-up spike. Simulation times: 300 ns (left), 270 ns (right).

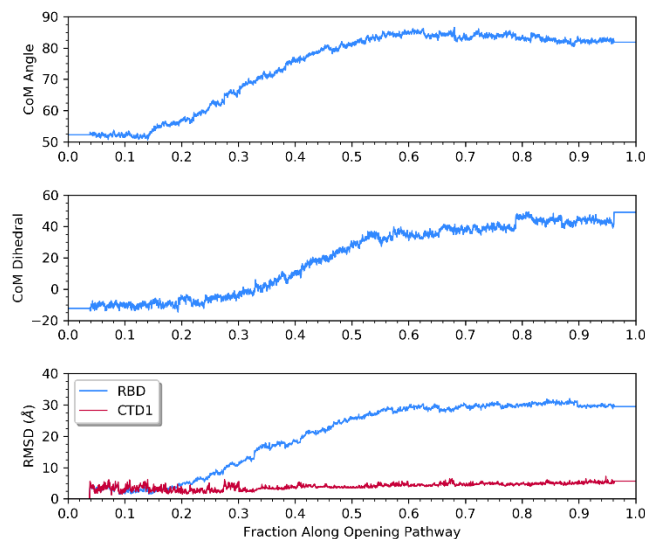


Figure S7. Spike structure properties during the RBD opening pathway, with the closed state on the left and the 1-up spike on the right. (Top) RBD opening angle, (middle) RBD rotation dihedral, (bottom) RMSD values for RBD and CTD1 domains, after best-fit to central helices (CH).

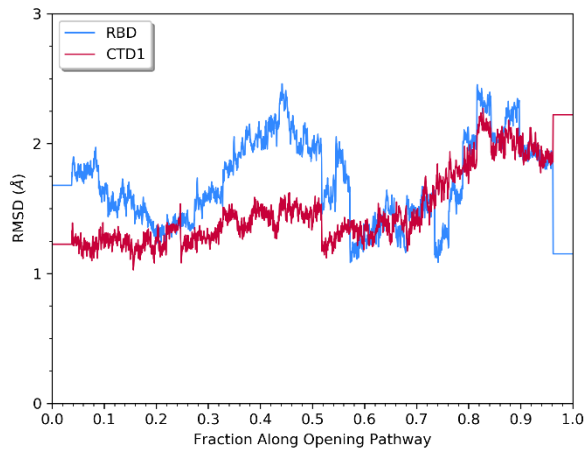


Figure S8. RMSD of RBD and CTD1 domains as a function of opening pathway, with each domain best-fit to the same atoms in the open reference model, using the residues listed in **Table S3**.

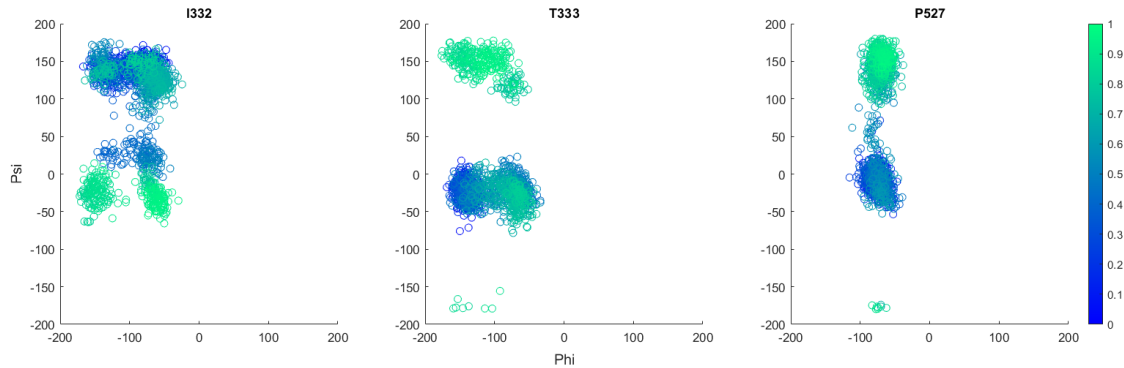


Figure S9. Selected backbone dihedrals in the RBD-CTD1 connector strands as a function of RBD opening pathway. Snapshots are shown as circles, with the opening progress indicated by the color range.

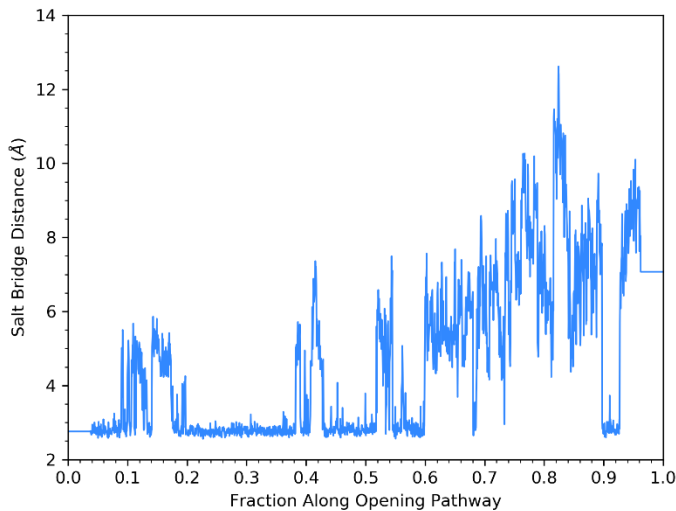


Figure S10. Distance between sidechains of K528 ($N\zeta$) and D389 ($C\delta$) as a function of RBD opening pathway.

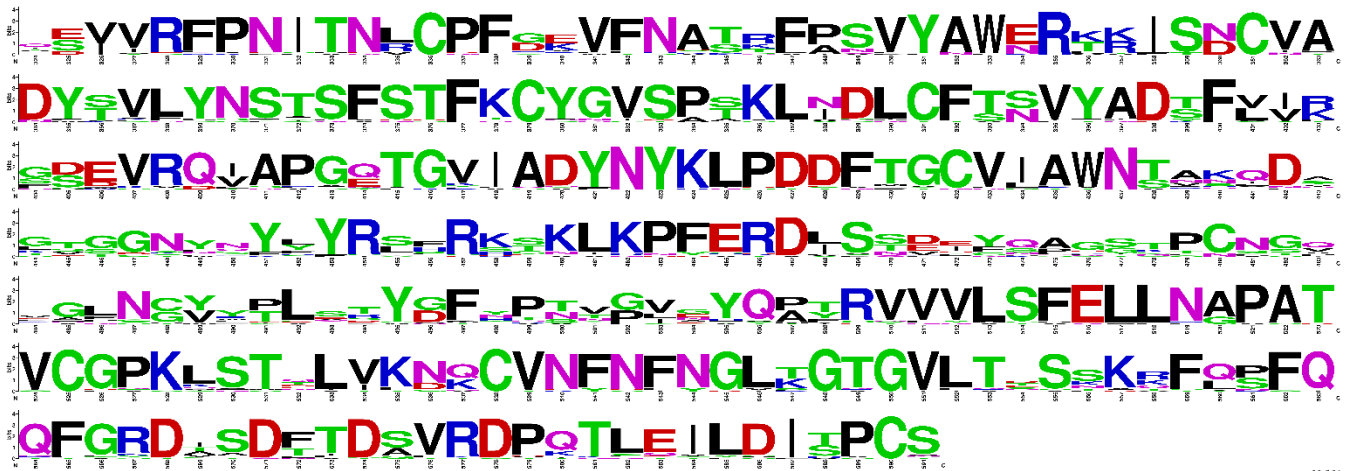


Figure S11. Sequence conservation for amino acids in the hinge pocket region (including positions 324-591), across 21 different coronaviruses.

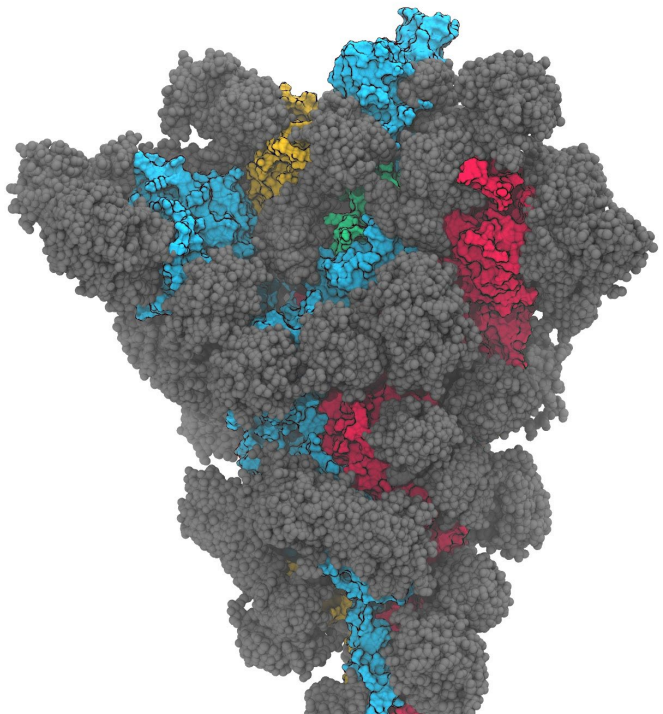


Figure S12. Spike structure in MD simulations, comparable to **Figure 3**. The gray glycans effectively shield the exterior of the conserved hinge region (highlighted in green).

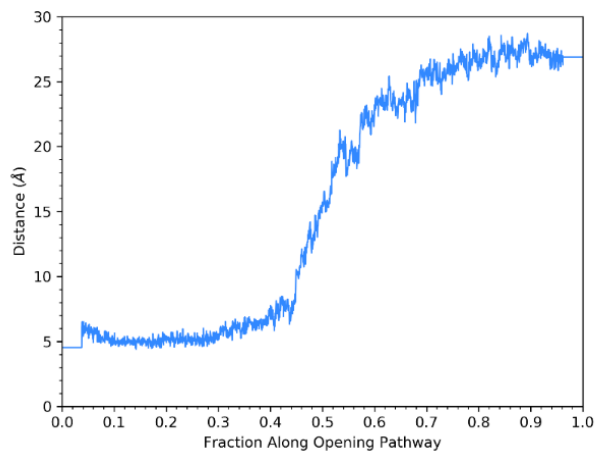


Figure S13. Distance between C_α atoms of A520 in RBD and Q564 in CTD1 as a function of RBD opening pathway for full spike;

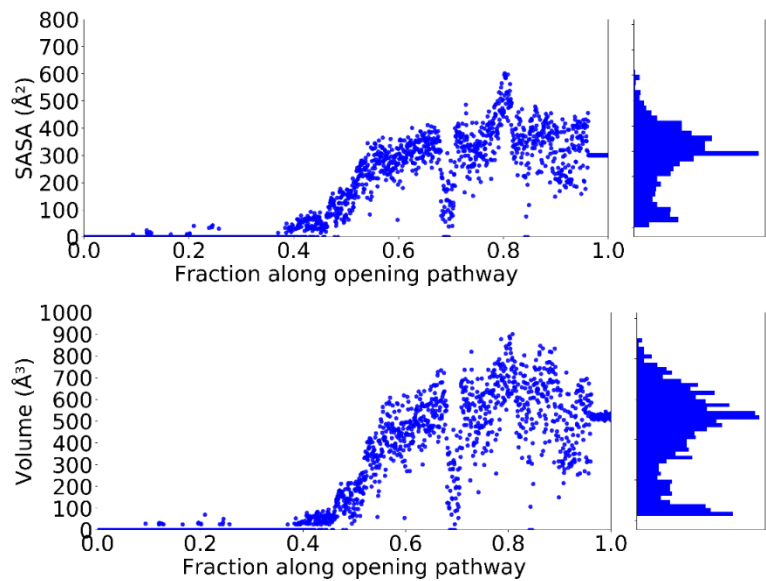


Figure S14: The change in hinge pocket volume and SASA as a function of RBD opening pathway. Data were calculated from the NEB snapshots using fpocket.¹

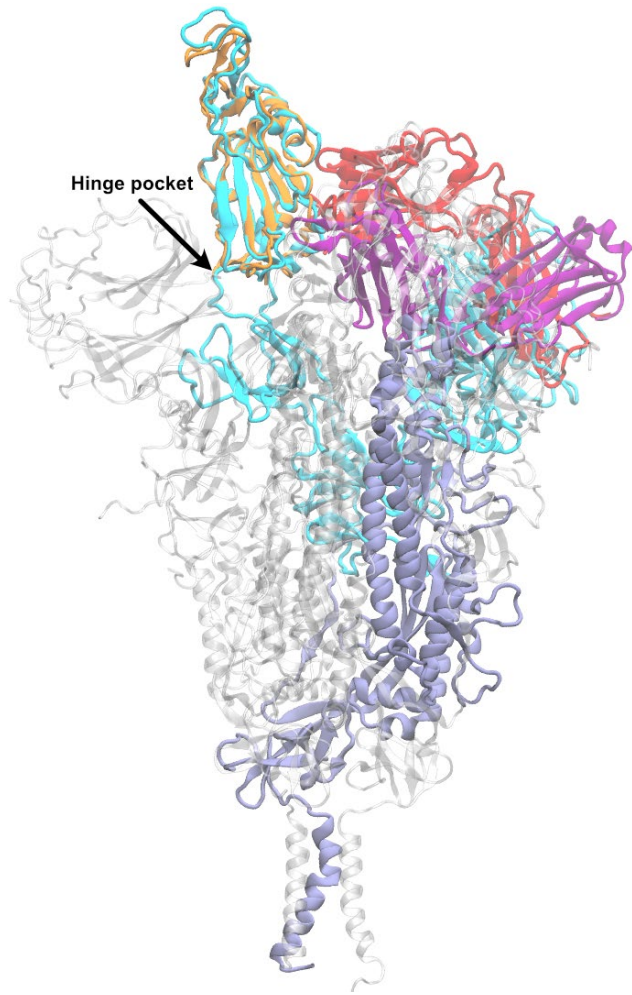


Figure S15. Spike protein from 1-up MD (1 protomer shown with S1 in cyan and S2 in gray, other protomers transparent), with hinge pocket indicated in relation to location of binding of cryptic antibody CR3022 from crystal structure 6W41² (RBD in orange, antibody in red/purple). The crystal structure contained only the RBD, not the entire spike. The RBD domains of the 2 systems were best-fit.

2. Tables

Table S1. Structures and types of glycans on each chain.³

Type	Chain A	Chain B	Chain C	Sequence
M5	N61, N122, N657	N61, N165, N122, N603, N709, N717, N1074	N61, N122, N603	aDMan(1→6)[aDMan(1→3)]aDMan(1→6) [aDMan(1→3)]bDMan(1→4)bDGlcNAc(1→4)bDGlcNAc(1→)
M6	N709, N801		N717	aDMan(1→6)[aDMan(1→3)]aDMan(1→6) [aDMan(1→2)aDMan(1→3)]bDMan(1→4)bDGlcNAc(1→4)bDGlcNAc(1→)
M7		N801		aDMan(1→2)aDMan(1→2)aDMan(1→3)[aDMan(1→6) [aDMan(1→3)]aDMan(1→6)]bDMan(1→4)bDGlcNAc(1→4)bDGlcNAc(1→)
M8	N234			aDMan(1→2)aDMan(1→6)[aDMan(1→3)]aDMan(1→6) [aDMan(1→2)aDMan(1→2)aDMan(1→3)]bDMan(1→4)bDGlcNAc(1→4)bDGlcNAc(1→)
M9		N234	N234	aDMan(1→2)aDMan(1→6)[aDMan(1→2)aDMan(1→3)]aDMan(1→6) [aDMan(1→2)aDMan(1→2)aDMan(1→3)]bDMan(1→4)bDGlcNAc(1→4)bDGlcNAc(1→)
A2	N616, N1158	N1098	N74, N282, N1158	bDGlcNAc(1→2)aDMan(1→6) [bDGlcNAc(1→2)aDMan(1→3)]bDMan(1→4)bDGlcNAc(1→4)bDGlcNAc(1→)
A3	N74			bDGlcNAc(1→6)[bDGlcNAc(1→2)]aDMan(1→6) [bDGlcNAc(1→2)aDMan(1→3)]bDMan(1→4)bDGlcNAc(1→4)bDGlcNAc(1→)
FA1	N1134	N343		bDGlcNAc(1→2)aDMan(1→3)[aDMan(1→6)]bDMan(1→4)bDGlcNAc(1→4) [aLFuc(1→6)]bDGlcNAc(1→)
FA2	N17, N331, N343, N603, N1098	N122, N331, N343, N616	N149, N343, N616, N709, N801, N1074, N1134	bDGlcNAc(1→2)aDMan(1→6)[bDGlcNAc(1→2)aDMan(1→3)]bDMan(1→4)bDGlcNAc(1→4)[aLFuc(1→6)]bDGlcNAc(1→)
FA2G2S1	N149, N1074	N1158	N165	aDNeu5Ac(2→6)bDGal(1→4)bDGlcNAc(1→2)aDMan(1→6) [bDGal(1→4)bDGlcNAc(1→2)aDMan(1→3)]bDMan(1→4)bDGlcNAc(1→4) [aLFuc(1→6)]bDGlcNAc(1→)
FA2G2S2	N165			xDNeu5Ac(2→6)bDGal(1→4)bDGlcNAc(1→2)aDMan(1→6) [aDNeu5Ac(2→6)bDGal(1→4)bDGlcNAc(1→2)aDMan(1→3)]bDMan(1→4)bDGlcNAc(1→4) [aLFuc(1→6)]bDGlcNAc(1→)
FA3	N282	N17, N149, N1134	N17	bDGlcNAc(1→6)[bDGlcNAc(1→2)]aDMan(1→6) [bDGlcNAc(1→2)aDMan(1→3)]bDMan(1→4)bDGlcNAc(1→4)[aLFuc(1→6)]bDGlcNAc(1→)

FA3G3S1		N282	N331	aDNeu5Ac(2→6)bDGal(1→4)bDGlcNAc(1→2)aDMan(1→3)[bDGal(1→4)bDGlcNAc(1→6) [bDGal(1→4)bDGlcNAc(1→2)]aDMan(1→6)]bDMan(1→4)bDGlcNAc(1→4) [aLFuc(1→6)]bDGlcNAc(1→)
FA3G3S2		N74		aDNeu5Ac(2→6)bDGal(1→4)bDGlcNAc(1→6)[bDGal(1→4)bDGlcNAc(1→2)]aDMan(1→6) [aDNeu5Ac(2→6)bDGal(1→4)bDGlcNAc(1→2)aDMan(1→3)]bDMan(1→4)bDGlcNAc(1→4) [aLFuc(1→6)]bDGlcNAc(1→)
FA4	N1173	N1173	N1173	bDGlcNAc(1→6)[bDGlcNAc(1→2)]aDMan(1→6)[bDGlcNAc(1→4) [bDGlcNAc(1→2)]aDMan(1→3)]bDMan(1→4)bDGlcNAc(1→4)[aLFuc(1→6)]bDGlcNAc(1→)
FA4G4S1	N1194	N1194	N1194	aDNeu5Ac(2→6)bDGal(1→4)bDGlcNAc(1→6)[bDGal(1→4)bDGlcNAc(1→2)]aDMan(1→6) [bDGal(1→4)bDGlcNAc(1→4) [bDGal(1→4)bDGlcNAc(1→2)]aDMan(1→3)]bDMan(1→4)bDGlcNAc(1→4) [aLFuc(1→6)]bDGlcNAc(1→)
Hybrid G1	N717	N657	N657	bDGal(1→4)bDGlcNAc(1→2)aDMan(1→3)[aDMan(1→6) [aDMan(1→3)]aDMan(1→6)]bDMan(1→4)bDGlcNAc(1→4)bDGlcNAc(1→)
Hybrid G1S1			N1098	aDNeu5Ac(2→6)bDGal(1→4)bDGlcNAc(1→2)aDMan(1→3)[aDMan(1→6) [aDMan(1→3)]aDMan(1→6)]bDMan(1→4)bDGlcNAc(1→4)bDGlcNAc(1→)
O1		T323		bDGal(1→3)aDGalNAc(1→)
O2	T323, S325			aDNeu5Ac(2→3)bDGal(1→3)aDGalNAc(1→)
O3		T323		aDNeu5Ac(2→3)bDGal(1→3)[aDNeu5Ac(2→6)]aDGalNAc(1→)

Table S2. Disulfide bonds in the “amended models”. Rows in bold indicate the five disulfide bonds in the RBD and CTD1 domains, also included in the RBD+CTD1 construct.

SARS-CoV-2
C131 - C166
C291 - C301
C336 - C361
C379 - C432
C391 - C525
C480 - C488
C538 - C590
C617 - C649
C662 - C671
C730 - C768
C743 - C749
C1032 - C1043
C1082 - C1126

Table S3. Reside ranges used for RMSD calculations

Subunit	Domain/ Region of interest	Residues in domain	Residues for RMSD
S1	NTD	16-285	27-66, 81-140, 164-172, 186-196, 200-211, 215-242, 263-285
	RBD	335-530	335-454, 462-466, 491-515, 522-530
	CTD1	315-334, 531-591	315-334, 531-591
	CTD2	592-685	592-620, 641-676
S2	UH	686-813	691-811, 813
	S2' (KRSF)	814-817	814-817
	FP	818-825	818-825
	HR1	867-984	867-984
	CH	985-1036	985-1036
	CD	1037-1137	1037-1137

Table S4. Amino acids used to define center-of-mass collective variables for the RBD closed-open transition. The group is defined by the center of mass of all C α atoms of all amino acids in the range.

CoM groups	1	2	3	4
Angle	F338-L517	E324-V327, C538-L585	T747*-Q755*	
Dihedral	E324-V327, C538-F543, L546-T549	A575-D578, L582-D586	N354-I358, T396-S399	S375-C379, C432-W436

Asterisks indicates the neighboring protomer on the clockwise side when viewing the spike from the S1 side (top side)

Table S5. List of sequences used to calculate conservation scores. We gratefully acknowledge the following Authors from the Originating laboratories responsible for obtaining the specimens and the Submitting laboratories where genetic sequence data were generated and shared via the GISAID Initiative, on which this research is based. All submitters of data may be contacted directly via www.gisaid.org⁴

Accession ID	Virus Name	Location	Date Collected	Host	Originating Lab	Submitting Lab	Authors
EPI_ISL_4021-24	hCoV-19/Wuhan/WIV04/2019 (SARS-CoV-2)	Asia / China / Hubei / Wuhan	2019-12-30	<i>Homo sapiens</i>	Wuhan Jinyintan Hospital	Wuhan Institute of Virology, Chinese Academy of Sciences	Peng Zhou, Xing-Lou Yang, Ding-Yu Zhang, Lei Zhang, Yan Zhu, Hao-Rui Si, Zhengli Shi

EPI_ISL_4105 39	hCoV-19/pangolin/Guangxi/P1E /2017	Asia / China / Guangxi	2017	Manis javanica	Beijing Institute of Microbiology and Epidemiology	Beijing Institute of Microbiology and Epidemiology	Wu-Chun Cao; Tommy Tsan-Yuk Lam; Na Jia; Ya-Wei Zhang; Jia-Fu Jiang; Bao-Gui Jiang
EPI_ISL_4105 41	hCoV-19/pangolin/Guangxi/P5E /2017	Asia / China / Guangxi	2017	Manis javanica	Beijing Institute of Microbiology and Epidemiology	Beijing Institute of Microbiology and Epidemiology	Wu-Chun Cao; Tommy Tsan-Yuk Lam; Na Jia; Ya-Wei Zhang; Jia-Fu Jiang; Bao-Gui Jiang
EPI_ISL_4105 40	hCoV-19/pangolin/Guangxi/P5L/ 2017	Asia / China / Guangxi	2017	Manis javanica	Beijing Institute of Microbiology and Epidemiology	Beijing Institute of Microbiology and Epidemiology	Wu-Chun Cao; Tommy Tsan-Yuk Lam; Na Jia; Ya-Wei Zhang; Jia-Fu Jiang; Bao-Gui Jiang
EPI_ISL_4105 38	hCoV-19/pangolin/Guangxi/P4L/ 2017	Asia / China / Guangxi	2017	Manis javanica	Beijing Institute of Microbiology and Epidemiology	Beijing Institute of Microbiology and Epidemiology	Wu-Chun Cao; Tommy Tsan-Yuk Lam; Na Jia; Ya-Wei Zhang; Jia-Fu Jiang; Bao-Gui Jiang
EPI_ISL_4105 42	hCoV-19/pangolin/Guangxi/P2V /2017	Asia / China / Guangxi	2017	Manis javanica	Beijing Institute of Microbiology and Epidemiology	Beijing Institute of Microbiology and Epidemiology	Wu-Chun Cao; Tommy Tsan-Yuk Lam; Na Jia; Ya-Wei Zhang; Jia-Fu Jiang; Bao-Gui Jiang
EPI_ISL_4107 21	hCoV-19/pangolin/Guangdong/ 1/2019	Asia / China / Guangdong	2019	Manis javanica	South China Agricultural University	South China Agricultural University	Yongyi Shen, Lihua Xiao, Wu Chen
NC_019843.3	Middle East respiratory syndrome-related coronavirus			<i>Homo sapiens</i>			van Boheemen,S., de Graaf,M., Lauber,C., Bestebroer,T.M., Raj,V.S., Zaki,A.M., Osterhaus,A.D., Haagmans,B.L., Gorbalenya,A.E., Snijder,E.J. and Fouchier,R.A.
NP_073551.1	Human coronavirus 229E			<i>Homo sapiens</i>			Thiel,V., Herold,J. and Siddell,S.G.

YP_00955524 1.1	Human coronavirus OC43			<i>Homo sapiens</i>			St-Jean,J.R., Jacomy,H., Desforges,M., Vabret,A., Freymuth,F. And Talbot,P.J.
AVP78042.1	Bat SARS-like coronavirus			<i>Rhinolophus pusillus</i>			Hu,D., Zhu,C., Ai,L., He,T., Wang,Y., Ye,F., Yang,L., Ding,C.,Zhu,X., Lv,R., Zhu,J., Hassan,B., Feng,Y., Tan,W. and Wang,C.
APO40579.1	Severe acute respiratory syndrome-related coronavirus			<i>Rhinolophus sp.</i>			Tao,Y. and Tong,S.
YP_00385858 4.1	Bat coronavirus BM48-31/BGR/2008			<i>Rhinolophus blasii</i>			Drexler,J.F., Corman,V.M. and Drosten,C.
AHX37558.1	<i>Rhinolophus affinis</i> <i>Coronavirus</i>			<i>Rhinolophus affinis</i>			He,B., Zhang,Y., Xu,L., Yang,W., Yang,F., Feng,Y., Xia,L., Zhou,J., Zhen,W., Feng,Y., Guo,H., Zhang,H. and Tu,C.
AAZ67052.1	Bat Coronavirus RaTG13			<i>Bat</i>			Li,W., Shi,Z., Yu,M., Ren,W., Smith,C., Epstein,J.H., Wang,H.,Crameri,G., Hu,Z., Zhang,H., Zhang,J., McEachern,J., Field,H.,Daszak,P., Eaton,B.T., Zhang,S. and Wang,L.F.
ABD75332.1	Bat SARS CoV Rm1/2004			<i>Rhinolophus macrotis</i>			Li,W., Shi,Z., Yu,M., Ren,W., Smith,C., Epstein,J.H., Wang,H., Crameri,G., Hu,Z., Zhang,H., Zhang,J., McEachern,J., Field,H., Daszak,P., Eaton,B.T., Zhang,S. and Wang,L.F.
YP_00982505 1.1	SARS Coronavirus			<i>Homo sapiens</i>			He,R., Dobie,F., Ballantine,M.,

						Leeson,A., Li,Y., Bastien,N., Cutts,T., Andonov,A., Cao,J., Booth,T.F., Plummer,F.A., Tyler,S., Baker,L. and Li,X.
ATO98108.1	Bat SARS-like Coronavirus			<i>Aselliscus stoliczkanu</i>		Hu,B., Zeng,L.P., Yang,X.L., Ge,X.Y., Zhang,W., Li,B., Xie,J.Z., Shen,X.R., Zhang,Y.Z., Wang,N., Luo,D.S., Zheng,X.S., Wang,M.N., Daszak,P., Wang,L.F., Cui,J. and Shi,Z.L.
ATO98145.1	Bat SARS-like Coronavirus			<i>Rhinolophus ferrumequinum</i>		Hu,B., Zeng,L.P., Yang,X.L., Ge,X.Y., Zhang,W., Li,B., Xie,J.Z., Shen,X.R., Zhang,Y.Z., Wang,N., Luo,D.S., Zheng,X.S., Wang,M.N., Daszak,P., Wang,L.F., Cui,J. and Shi,Z.L.
ATO98157.1	Bat SARS-like Coronavirus			<i>Rhinolophus sinicus</i>		Hu,B., Zeng,L.P., Yang,X.L., Ge,X.Y., Zhang,W., Li,B., Xie,J.Z., Shen,X.R., Zhang,Y.Z., Wang,N., Luo,D.S., Zheng,X.S., Wang,M.N., Daszak,P., Wang,L.F., Cui,J. and Shi,Z.L.
AAY88866.1	Bat SARS Coronavirus HKU3-1			<i>Bat</i>		Lau,S.K., Woo,P.C., Li,K.S., Huang,Y., Tsoi,H.W., Wong,B.H., Wong,S.S., Leung,S.Y., Chan,K.H. and Yuen,K.Y.
AGC74165.1	Bat Coronavirus Rp/Shaanxi2011			<i>Rhinolophus pusillus</i>		Yang,L., Wu,Z., Ren,X., Yang,F., He,G., Zhang,J., Dong,J., Sun,L., Zhu,Y., Du,J., Zhang,S. and Jin,Q.

AGC74176.1	Bat Coronavirus Cp/Yunnan2011			<i>Chaerephon plicata</i>			Yang,L., Wu,Z., Ren,X., Yang,F., He,G., Zhang,J., Dong,J., Sun,L., Zhu,Y., Du,J., Zhang,S. and Jin,Q.
AID16716.1	Bat SARS-like coronavirus			<i>Rhinolophus monoceros</i>			Lin,X.D., Wang,W., Hao,Z.Y., Wang,Z.X., Guo,W.P., Guan,X.Q., Wang,M.R., Wang,H.W., Zhou,R.H., Li,M.H., Tang,G.P., Wu,J., Holmes,E.C. and Zhang,Y.Z.
AIA62277.1	BtRf-BetaCoV/JL2012			<i>Rhinolophus ferrumequinum</i>			Wu,Z., Yang,L., Ren,X., He,G., Zhang,J., Yang,J., Qian,Z., Dong,J., Sun,L., Zhu,Y., Du,J., Yang,F., Zhang,S. and Jin,Q.
AIA62310.1	BtRs-BetaCoV/HuB2013			<i>Rhinolophus sinicus</i>			Wu,Z., Yang,L., Ren,X., He,G., Zhang,J., Yang,J., Qian,Z., Dong,J., Sun,L., Zhu,Y., Du,J., Yang,F., Zhang,S. and Jin,Q.
QHR63300.2	Bat Coronavirus RaTG13			<i>Rhinolophus affinis</i>			Zhou,P., Yang,X.-L., Wang,X.-G., Hu,B., Zhang,L., Zhang,W., Si,H.-R., Zhu,Y., Li,B., Huang,C.-L., Chen,H.-D., Chen,J., Luo,Y., Guo,H., Jiang,R.-D., Liu,M.-Q., Chen,Y., Shen,X.-R., Wang,X., Zheng,X.-S., Zhao,K., Chen,Q.-J., Deng,F., Liu,L.-L., Yan,B., Zhan,F.-X., Wang,Y.-Y., Xiao,G.-F. and Shi,Z.-L.
AVP78031.1	Bat SARS-like Coronavirus			<i>Rhinolophus pusillus</i>			Hu,D., Zhu,C., Ai,L., He,T., Wang,Y., Ye,F., Yang,L., Ding,C., Zhu,X., Lv,R., Zhu,J.,

Table S6. Calculated sequence conservation percentages, across 28 coronavirus sequences, for the RBD and CTD1.

position	% conserved	sequence (SARS-CoV-2 listed first)
324	7.	EIIIIIEGVAQTTKQQGQVKQQTQVQDQ
325	43.	SSSSSSSSSDSEEEEDEDEEEDEESS
326	36.	IIIIIIVIVIVVVVVVVVVVVVVVVIV
327	79.	VVVVVVVVVYVVVVIVVVVVIVIIAVVV
328	93.	RRRRRRRESRRRRRRRRRRRRRRRRRRR
329	89.	FFFFFFFQLRFFFFFFFFFFFFFFFFF
330	93.	PPPPPPPAPKPPPPPPPPPPPPPPPP
331	89.	NNNNNNNE-PNNNNNNNNNNNNNNNNNN
332	89.	IIIIIIG-LIIIIIIIIIIIIIIII
333	89.	TTTTTTTV-PTTTTTTTTTTTTTTT
334	89.	NNNNNNNE-NNNQNNNNNNNNNNNNN
335	50.	LLLLLL---VLLRLRLLRRRRVRLV
336	96.	CCCCCCCC-CCCCCCCCCCCCCCCC
337	89.	PPPPPPPD-NPPPPPPPPPPPPPPPP
338	93.	FFFFFFF-IFFFFFFFFFFFFFFF
339	43.	GGGGGGGS-EHNGDDGDDGDDDDGH
340	43.	EEEEEEEP-AKQEEKKEKAEKRKREK
341	93.	VVVVVVVLVWVVVVVVVVVVVVVVVV
342	89.	FFFFFFFLYLFFFFFFFFFFFFFF
343	93.	NNNNNNNSHNNNNNNNNNNNNNNNN
344	82.	AAAAAAAGKDAIAAAAAAAAAAVAAA
345	61.	TSSSSSTTHKTSTTSTTTTSTTSTT
346	46.	RKKKKKT-TSRNSTRRKRRRRRRTR
347	93.	FFFFFFFVFFFFFFFFFFFFFFF
348	29.	AAAAAAAPIPPPPPPPPPPPPPAP
349	79.	SSSSSSQVSSSSNNSSSNSSSS
350	93.	VVVVVVVLVWVVVVVVVVVVVVVV
351	96.	YYYYYYYYYYLYYYYYYYYYYYYYYY
352	89.	AAAAAAAN-AAAAAANAAAAAANAAA
353	93.	WWWWWWWF-WWWWWWWWWWWWWWW
354	29.	NNNNNNNK-EEEEEEEEEEENE
355	96.	RRRRRRRR-RRRRRRRRRRRRRRR
356	43.	KKKKKKKL-KTLMKTTKTVKTTTTKT
357	43.	RRRRRRRV-TKRRRKKKRKKKRK
358	89.	IIIIIIF-FIIIIIIIIIIIIII

359	89.	SSSSSSST-SSSTSSSSSSSSSSSSSS
360	54.	NNNNNNNN-NDDNNDDNDNNDDDDND
361	96.	CCCCCCCC-CCCCCCCCCCCCCCCC
362	82.	VVVVVVVN-NIVVVVVVVVVVVVVVI
363	89.	AAAAAAAYVAAAAAAAAAAAAAAA
364	93.	DDDDDDDDNDNDDDDDDDDDDDDDD
365	89.	YYYYYYYLFMYYYYYYYYYYYYYYYY
366	46.	SSSSSSSTKSTASTTSTTSTTTTST
367	86.	VVVVVVKPSVVVVVVVVAVVVVVVV
368	82.	LLLLLLLQLFLLLLLFLLLLFLF
369	89.	YYYYYYYLSMYYYYYYYYYYYYYYYY
370	89.	NNNNNNNSGSNNNNNNNNNNNNNNNN
371	89.	SSSSSSSLGFSSSSSSSSSSSSSSSS
372	7.	ATTTTTFGITSATTTTTTTTTTT
373	89.	SSSSSSS-QSSSSSFSSSSSSSSSS
374	89.	FFFFFFFV-AFFFFFFFFFFFFFFF
375	89.	SSSSSSN-DSSSSSSSSSSSSSSSS
376	89.	TTTTTTD-STTTTTTTTTTTTTTT
377	96.	FFFFFFF-FFFFFFFFFFFFFFFF
378	86.	KKKKKKKTKKQKKKKKKKKKKKKKK
379	100.	CCCCCCCCCCCCCCCCCCCCCCCCCCC
380	89.	YYYYYYYSFNYYYYYYYYYYYYYYYY
381	89.	GGGGGGQNNGGGGGGGGGGGGGGG
382	89.	VVVVVVICIVVVVVVVVVVVVVVV
383	93.	SSSSSSSYDSSSSSSSSSSSSSSSS
384	86.	PPPPPPPPPAPPAPPAPPAPPAPP
385	43.	TTTTTTAAASTTISSTSSTSSSTS
386	93.	KKKKKKKAGKKKKKKKKKKKKKKKK
387	89.	LLLLLLLI-ILLLLLLLLLLLLLLL
388	46.	NNNNNNNAVYINNNIINIINIIINI
389	89.	DDDDDDDSNGDDDDDDDDDDDDDD
390	89.	LLLLLLNIMLLLLLLLLLLLLLLL
391	96.	CCCCCCCTCCCCCCCCCCCCCCCC
392	93.	FFFFFFYLFFFFFFFFFFFFFFF
393	71.	TTTTTTSASTSSSTTSTTTTTTT
394	43.	NNNNNNNSSSSNSSNSNSNSNS
395	89.	VVVVVVL-IVVVVVVVVVVVVVVV
396	89.	YYYYYYYIFTYYYYYYYYYYYYYYY
397	89.	AAAAAAALNIAAAAAAAAALNIA
398	96.	DDDDDDDEDDDDDDDDDDDDDD
399	39.	SSSSSSYTKEYSTTSTTTTST
400	96.	FFFFFFF-FFFFFFFFFFFFFFF

401	46.	VVVVVVVVS-ALVVVLLVLLVLLLLLVL
402	54.	IIVVVVVY-IIVVVIIVIIVIIIIII
403	50.	RKKKKRKPKRKKRRKRRKRRRRRRTR
404	50.	GGGGGGGLGNFGGGSSGSFGSSFSFGF
405	46.	DDDDDDDSPGSDDDSSDSSDSSSSSDS
406	71.	EEEEEEEMLREDDDEEDEEDEEEEEE
407	89.	VVVVVVVVKCKVVVVVVVVVVVVVVVV
408	89.	RRRRRRRSVVRRRRRRRRRRRRRRRRR
409	89.	QQQQQQQDDQQQQQQQQQQQQQQQQQ
410	50.	IIIIIILTVIIIVVIVVIVVIVVIV
411	89.	AAAAAAASSQAAAAAAAAAAAAAAA
412	89.	PPPPPPPVLPPPPPPPPPPPPPPPP
413	86.	GGGGGGGSFGGAAGGGGGGGGGGGGG
414	57.	QQQQQQQSTNQQQEEQEEQEEQEQQ
415	93.	TTTTTTATLTTTTTTTTTTTTTTTT
416	96.	GGGGGGGGKGGGGGGGGGGGGGGGGG
417	7.	KVVVVVRPYYVVVVVVVVVVVVVVKV
418	93.	IIIIIIVLIIIIIIIIIIIIIIII
419	93.	AAAAAAASAQAAAAAAAAAAAAAAA
420	89.	DDDDDDDDQVSDDDDDDDDDDDDDDDD
421	93.	YYYYYYYFYFYYYYYYYYYYYYYYY
422	96.	NNNNNNNN-NNNNNNNNNNNNNNNNNN
423	96.	YYYYYYYY-YYYYYYYYYYYYYYYYYY
424	93.	KKKKKKKK-RKKKKKKKKKKKKKKKK
425	89.	LLLLLLQ-ILLLLLLLLLLLLLLL
426	89.	PPPPPPPS-DPPPPPPPPPPPPPPP
427	89.	DDDDDDDF-TDDDDDDDDDDDDDDDD
428	86.	DDDDDDDS-TDDDDDDDDDDDDDEDDDD
429	89.	FFFFFFN-AFFFFFFFFFFFFFFFF
430	79.	TTTTTTTP-TTTMTTMTTLTTTITTT
431	89.	GGGGGGGTASGGGGGGGGGGGGGGGG
432	96.	CCCCCCCCNCCCCCCCCCCCCCCCC
433	93.	VVVVVVVLVQVVVVVVVVVVVVVVVV
434	79.	IIIIIIIGLILILIILIIIIIIII
435	89.	AAAAAAALRYAAAAAAAAAAAAAAA
436	93.	WWWWWWAWYWWWWWWWWWWWWWWWW
437	93.	NNNNNN--NNNNNNNNNNNNNNNNNN
438	29.	SSSSSSV--TTTTTTTTTTTST
439	18.	NVVVVVNPA PAN NRA ARAA AAAA AKA
440	21.	NKKKKKNHSAKSSNKQNQSKNNKKHK
441	11.	LQQQQQLNIAQVLIQQIQQKHQQQQQIQ
442	89.	DDDDDDDLNNDDDDDDDDDDDDDDDD

443	18.	SAAAAASTVTSSAQAKVSTQRIVTAV
444	14.	KLLLLLKTGSGK-TGGTGGSGGGGGKG
445	11.	VTTTTTVI-V-S-S--S---T-----E-
446	29.	GGGGGGGT-S---S---T--S-----G-
447	36.	GGDGGGG--S---G--G--G-----G-
448	43.	NNNNNNNKNT-GSN--N--N-----N-
449	32.	YYYYYYYPCW-NNF--Y--Y-----F-
450	39.	N-GGGGNKPNHNENQQNQSNNQQNSYNN
451	82.	Y-YYYYYYYFKYFYFYYYYYYYYYYYYYY
452	32.	LLLLLLSLSRFYFKYYKYFLYYYYFYLF
453	93.	YYYYYYYYYFFYYYYYYYYYYYYYYYYYY
454	89.	RRRRRRRI-GRRRRRRRRRRRRRRRRR
455	32.	LLLLLLLN-FSLRSSSYSSWSSSSSLS
456	36.	FFFFFFFK-IHFFLHYLSHVHSSHHFH
457	89.	RRRRRRRC-ERRRRRRRRRRRRRRRRR
458	57.	KKKKKKKS-DSHHHKHKSRKKKSCKS
459	39.	SSSSSSSRGSTGGTEGTSSTETTSTAT
460	11.	NKKKKKNLKVKKKKKKKKKKKKKKKKKK
461	86.	LLLLLLLVLFLIILLLLLLLLLLLLL
462	82.	KKKKKKK--KKKRKKRKKNKKKKKKKK
463	89.	PPPPPPPDNNPPPPPPPPPPPPPPPPP
464	82.	FFFFFFDF-FYYFFFFFYFFFFFFF
465	86.	EEEEEEERVHEEGEEEEEEEEEEEEE
466	89.	RRRRRRRTKDRRRRRRRRRRRRRRRR
467	89.	DDDDDDD--VDDDDDDDDDDDDDDDD
468	39.	IIIIIIVFYLILILLILLILLILL
469	89.	SSSSSSPGASSSSSSSSSSSSSSSS
470	29.	TTTTTTTQSQSNNNSSNSSSSSSTS
471	32.	EEEEEEELVHDVVVDDVDDDDDEDED
472	32.	IIIIIIIVCCELLPEEPEEIDEDEDIE
473	36.	YYYYYYYNNFF-YFF--F--YG--G-GY-
474	29.	QQQQQQQASK-NNS--S--S-----Q-
475	32.	AAAAAAANLA-SPP--P--P-----A-
476	32.	GGGGGGGQKP-ASD--D--G-----G-
477	29.	SSSSSSSYIK-GGG--G--G-----S-
478	25.	TTTTTTTS-N-GGK--K--Q-----K-
479	39.	PPPPPPPP-F-TTP--P--S-----P-
480	54.	CCCCCCCC-CNCCC--C--C-----CN
481	29.	NNNNNNNV-P-SS-----N-
482	36.	GGGGGGGS-CGS-T--T--S-----GG
483	14.	VQQQQQV---VIAP--P--A-----QV
484	11.	EVVVVVEIPKRSEP--P--I-----TR

485	39.	GGGGGGGVGL-QGA--A--G-----G-
486	11.	FLLLLLFPGN-LLF--L--P-----L-
487	79.	NNNNNNNSCG-GNNNNNNNNNNNNNNN-
488	46.	CCCCCCCCTA--CCCGGCGGCGGGGGC-
489	46.	YYYYYYYYVM--YYYVVYVVYVVVVVY-
490	7.	FYYYYYYFWP--EKWRYWRRNYYRYLYY-
491	46.	PPPPPPPPEISTPPPTPTTPTTTTTPT
492	89.	LLLLLLDVCLLLLLLLLLLLLLLLLLL
493	7.	QEEEEEQGAVSKANSSNSSRSSSSSYS
494	14.	SRRRRRSDNGTSSDTTDTTPTTTTTRT
495	93.	YYYYYYYYWSYYYYYYYYYYYYYYYYYY
496	50.	GGGGGGGQAGDGGGDDGDDGDDDDGD
497	89.	FFFFFFFWYPFFFFFFFFFFFFFFFFFF
498	4.	QHHHHHHLSGNTYYYYNFNYNNYN
499	71.	PPPPPPPV-KPPQTPPPTPPTPPPQPPP
500	46.	TTTTTTA-NNTSTSSTTNSSNNNTN
501	14.	NTTTTTNS-NVVSNVITVVAVVVVVDV
502	54.	GGGGGGGG-GPGGGPPGPPGPBPPGP
503	54.	VVVVVVVS-ILVIIIVVIILVVLVLVVL
504	32.	GNNNNNGTKGEGGAEGEDGADEAEAGE
505	82.	YYYYYYYYVYTYYFYYYYYYHYYYYYYH
506	89.	QQQQQQQAYCQQQQQQQQQQQQQQQQQ
507	50.	PPPPPPPMTPAPPPAAPAAPAAAAAPA
508	29.	YFFFFFYTIATYYTTYTYYTTTYT
509	89.	RRRRRRREGGRRRRRRRRRRRRRRRRR
510	89.	VVVVVVVQSTVVVVVVVVVVVVVVVVVV
511	89.	VVVVVVVLLNVVVVVVVVVVVVVVVVV
512	89.	VVVVVVVQYYVVVVVVVVVVVVVVVVVV
513	93.	LLLLLLMVLLLLLLLLLLLLLLLLLL
514	93.	SSSSSSSGSTSSSSSSSSSSSSSSSS
515	86.	FFFFF-F--PFFFFFFFFFFFFFFF
516	89.	EEEEEEE--QEEEEEEEEECCCCCCC
517	89.	LLLLLLL--ALLLLLLLLLLLLLLL
518	89.	LLLLLLL--FLLLLLLLLLLLLLLL
519	4.	HNNNNNN--LNNNNNNNNNNNNNNNNN
520	71.	AGGGGGA--GAAAAAAAAAAAAAAA
521	89.	PPPPPPP--WPPPPPPPPPPPPPPPP
522	89.	AAAAAAA--SAAAAAAAACAAAAAA
523	89.	TTTTTTT--DTTTTTTTTTTTTTT
524	89.	VVVVVVV--SVVVVVVVVVVVVVVV
525	93.	CCCCCCC--CCCCCCCCCCCCCCCCC
526	93.	GGGGGGGDGLGGGGGGGGGGGGGGGG

527	89.	PPPPPPPTVQPPPPPPPPPPPPPPPPPP
528	96.	KKKKKKKKSKKKKKKKKKKKKKKKKKKK
529	11.	KLLLLLQISALKQLLLLLLLLLLLLKL
530	89.	SSSSSSSAFNSSSSSSSSSSSSSSSSSS
531	93.	TTTTTTSMTTTTTTTTTTTTTTTTT
532	14.	NTTTTNQNDQEEDQQDGQDETSQOPENQ
533	89.	LLLLLL-VILLLLLLLLLLLLLLLLL
534	75.	VVVVVVV-TIVVVIVVIVVIVVIVVV
535	86.	KKKKKKKLLKKTKKKKKKKKKKKKKKK
536	71.	NDDDDNGDGNNNNNNNNNNNNNNNNNNN
537	39.	KKKKKKKNKVQKKQQQQQQQQQQQQQKQ
538	100.	CCCCCCCCCCCCCCCCCCCCCCCCCCCC
539	96.	VVVVVVVVTVVVVVVVVVVVVVVVVVV
540	93.	NNNNNNNEKNNNNNNNNNNNNNNNNNN
541	89.	FFFFFFFYYFFFFFFFFFFFFFFFF
542	93.	NNNNNNNSNDNNNNNNNNNNNNNNNNN
543	89.	FFFFFFFLILFFFFFFFFFFFFFFF
544	89.	NNNNNNNYYNNNNNNNNNNNNNNNNNN
545	96.	GGGGGGGGDGGGGGGGGGGGGGGGGGG
546	89.	LLLLLLLVVILLLLLLLLLLLLLLLLL
547	46.	TTTTTTSSLKTTKRTKTKKKKKTK
548	100.	GGGGGGGGGGGGGGGGGGGGGGGGGGG
549	89.	TTTTTTTRVQTTTTTTTTTTTTTTT
550	100.	GGGGGGGGGGGGGGGGGGGGGGGGGGG
551	96.	VVVVVVVVVIVVVVVVVVVVVVVVV
552	89.	LLLLLLFIFLLLLLLLLLLLLLLL
553	89.	TTTTTTQRVTTTTTTTTTTTTTTT
554	18.	ETTTTENVEDSNPETPDDSSADSDKED
555	93.	SSSSSSCSVSSSSSSSSSSSSSSSSS
556	14.	NKKKKKSTNNSTLSSSSSSSSSSNS
557	89.	KKKKKKADAKKKKKKKKKKKKKKKKK
558	25.	KQQQQQKVTRRKRRRRRRRKTRKR
559	93.	FFFFFFFGFYFFFFFFFFFFFFFFF
560	32.	LLLLLLVLYQQQQQQQQQQQQQQQQLQ
561	46.	PPPPPPPRNNSPPPSSPSSPSSSSPS
562	89.	FFFFFF--SFFFFFFFFFFFFFFF
563	96.	QQQQQQQQIQQQQQQQQQQQQQQQQQQ
564	89.	QQQQQQQRTNQQQQQQQQQQQQQQQQ
565	93.	FFFFFFFYLFFFFFFFFFFFFFFFF
566	89.	GGGGGGVTLGGGGGGGGGGGGGGGG
567	82.	RRRRRRRYSYKRRRRRRRRRRRRRK
568	96.	DDDDDDDDTDDDDDDDDDDDDDDDDDD

569	29.	IIIIIIIASSAVVFTTVTTVTAATATIA
570	11.	ASSSSSSAYGNSSSSSSSSSSSSSSSSAS
571	89.	DDDDDDDDQ--DDDDDDDDDDDDDDDDDD
572	29.	TTTTTTTLLNFFFFFFFFFIFTF
573	82.	TTTTTTTVLLITTTTTTTTTTTTTI
574	89.	DDDDDDD--YDDDDDDDDDDDDDDDDDD
575	29.	AAAAAAAGGGSSSSSSSSSSSSSSSSAS
576	89.	VVVVVVVVYFFVVVVVVVVVVVVVVVV
577	93.	RRRRRRRYKRRRRRRRRRRRRRRRRRRR
578	96.	DDDDDDDSDDDDDDDDDDDDDDDDDDDD
579	89.	PPPPPPPDVYPPPPPPPPPPPPPPPPP
580	71.	QQQQQQQQDTIQKKKQQKQQKQQQQQQQ
581	93.	TTTTTTNKTTTTTTTTTTTTTTTTTT
582	79.	LLLLLLL-GNLFLLLSLLSLLLLLLL
583	75.	EEEEEEE-TREEEEEEQDEEEQEQQEE
584	86.	IIIIIIYITIIIIVIIIVIIIIIIII
585	89.	LLLLLLYYFLLLLLLLLLLLLLLLLL
586	89.	DDDDDDDCSMDDDDDDDDDDDDDDDD
587	96.	IIIIIIILIIIIIIIIIIIIIIIIII
588	46.	TTTTTTTRTRTSASSSSTSSSSSSTT
589	93.	PPPPPPPAPSPPPPPPPPPPPPPPPP
590	100.	CCCCCCCCCCCCCCCCCCCCCCCCCCC
591	86.	SSSSSSSVNYSSSSSASSSSSSSSSS

REFERENCES

1. Le Guilloux, V.; Schmidtke, P.; Tuffery, P., Fpocket: An open source platform for ligand pocket detection. *BMC Bioinformatics* **2009**, *10* (1), 168.
 2. Yuan, M.; Wu, N. C.; Zhu, X.; Lee, C.-C. D.; So, R. T. Y.; Lv, H.; Mok, C. K. P.; Wilson, I. A., A highly conserved cryptic epitope in the receptor binding domains of SARS-CoV-2 and SARS-CoV. *Science* **2020**, *368* (6491), 630-633.
 3. Casalino, L.; Gaieb, Z.; Goldsmith, J. A.; Hjorth, C. K.; Dommer, A. C.; Harbison, A. M.; Fogarty, C. A.; Barros, E. P.; Taylor, B. C.; McLellan, J. S.; Fadda, E.; Amaro, R. E., Beyond Shielding: The Roles of Glycans in the SARS-CoV-2 Spike Protein. *ACS Central Science* **2020**, *6* (10), 1722-1734.
 4. Elbe, S.; Buckland-Merrett, G., Data, disease and diplomacy: GISAID's innovative contribution to global health. *Global Challenges* **2017**, *1* (1), 33-46.